Registration of Sparse-Dense Point Cloud from LiDAR and its Applications

Surbhi Barnwal*, Salil Goel, & Mansi P. Koshti

Department of Civil Engineering, IIT Kanpur, Kanpur, India
*Corresponding Author's email: surbhib20@iitk.ac.in

Abstract

Point cloud registration is a crucial fundamental task in computer vision and robotics. Accurate alignment of point clouds is a basis for numerous applications such as 3D reconstruction, object recognition, autonomous navigation, environmental mapping, landslide monitoring, precision forestry, etc. The principle of point cloud registration is to find the best transformation matrix that best aligns two consecutive scans, and based on the transformation matrices, all the scans are merged, and a new complete 3D point cloud of the scene is created. Multiple registration algorithms, such as those based on Iterative Closest Point (ICP), feature-based, and deep learning-based algorithms have been proposed in the literature. However, all such algorithms assume the point clouds to be captured from similar sensors with similar quality. Registration of point clouds captured from different types of sensors is typically challenging. It poses various problems, including extraction of reliable features, accurate feature matching, and the absence of a sufficient number of features (typically in the case of sparse point cloud). This paper proposes a novel point cloud registration pipeline that allows the registration of a dense point cloud, typically captured from an expensive LiDAR sensor with a sparse point cloud, typically captured using a relatively inexpensive LiDAR sensor. The proposed pipeline is verified through multiple experiments, and its performance is evaluated. Although the proposed approach currently relies on various manual procedures, most can be easily automated. The potential applications of sparse–dense point cloud registration is extensive, including automatic updating of 3D buildings, heritage mapping, and calibration of two sensors based on sparse data. This paper highlights the challenges in such a sparse-dense point cloud registration, including finding sufficient corresponding point pairs and feature matching.

Keywords: Point cloud registration; LiDAR; ICP

Introduction

The process of aligning three-dimensional (3D) point clouds (often referred to as "Point Cloud Registration") is a crucial initial step in numerous applications related to 3D modelling and mapping including fields of photogrammetry, computer vision, precision forestry, environmental monitoring, and robotics, archaeology for the better visualization and analysis (Sanchez et al., 2017; De Reu et al., 2014). Point cloud registration is a method of aligning two or more-point clouds collected from one or different types of sensors from different parts of the same scene (Brightman et al., 2023). This procedure involves the transformation of point clouds into common coordinates using a transformation matrix. The need to register two or more-point clouds arises from the limited field of view of a single scan recorded by a LiDAR sensor, which cannot capture the entire scene simultaneously (Huang et al., 2021). Registration tasks often pose challenges due to factors such as the complexity of the environmental scene, data sparsity, and the specific algorithms used (N. Xu et al., 2023). Point cloud registration may appear deceptively simple, yet numerous factors significantly impact its accuracy. These factors encompass collecting point clouds at different times, resulting in noise within the dataset, the complexity of the scene, the sparsity of the captured point cloud data, and the choice of algorithms utilized(Huang et al., 2021). Traditional methods for point cloud registration often rely on marker-based registration, where markers must be manually placed and transported. However, this approach is expensive, laborious, and time-consuming, making it an impractical option for registering multiple scans in unstructured environments (Wang et al., 2023). To address these challenges, researchers have introduced various marker-free registration techniques that offer increased efficiency, robustness, and reduced time requirements in such settings (Kelbe et al., 2016; X. Xu et al., 2022; Brenner et al., 2008). One widely adopted solution for point cloud registration is the Iterative Closest Point (ICP) algorithm (Besl & McKay, 1992). The main advantage of the ICP algorithm is its ability to perform point cloud registration without the requirement for artificial targets. Additionally, its iterative nature enhances efficiency and accuracy as it refines the solution over multiple iterations (He et al., 2021). However, there are a few drawbacks of the ICP algorithm, as its runtime is high, the overlap between the two scans should be high to run the operation, easily falls into local minima, and it is difficult to find complex features (S. Li et al., 2016). S. Li et al. (2016) Recently, ICP has undergone significant developments to improve its efficiency and accuracy by modifying the algorithm. These modifications include increasing the registration accuracy, reducing the runtime of the algorithm by limiting the number of points involved in the operation, implementing an optimization technique, and minimizing the overlap ratio (Han et al., 2016; W. Li & Song, 2015; Yang et al., 2016). Various feature-based algorithms are developed to eliminate the manual task of initialization as required in ICP, which is quite helpful for natural scene registration as it can detect and match distinctive features in the point cloud (Kelbe et al., 2016). These registration algorithms rely on the utilization of features, which are specific points that can be easily distinguished by their geometrical characteristics, such as position, local information content, and mathematical definition with respect to other points. An effective feature exhibits stability and distinctiveness, meaning the identified features should maintain consistency across all frames. Moreover, these features should be robust enough to be unaffected by external factors such as noise in the dataset variation in scale (Li et al., 2020). Most of the researchers focused on addressing the point cloud registration problem pertaining to the point cloud collected from a single sensor. This involves the alignment of either a dense point cloud or registration of a dense point cloud (Agamennoni et al., 2016; Bellekens et al., 2014; Pomerleau et al., 2015). Recently, there has been a growing demand for the registration of point clouds that vary in density, necessitated by the distinct benefits offered by different sensors as it has numerous applications. Sparse-dense point cloud registration holds significant potential for many applications, including automatically updating 3D buildings, heritage mapping, localization problem, and sensor calibration based on sparse data (Lamine Tazir et al., 2018). Leveraging one sensor's strengths to complement another's weaknesses has driven the need for sparse-dense point cloud registration. In addition to their benefits, sparse-dense point cloud registration presents particular challenges. These challenges arise from variations in point cloud density between the source and target point clouds, making it challenging to establish corresponding pairs and often resulting in incomplete registrations. Hence, one key factor to consider is the variation in sampling density during sparse, dense point cloud registration. This variation directly impacts the number of points in the point cloud and the spacing between them. When capturing the same part of the scanning environment from two distinct viewpoints, the dense point cloud will contain a more significant number of points arranged at a closer proximity, in contrast to the sparser point cloud. The variation in data density within the point cloud to be registered significantly impacts the geometric properties of individual points. This requires employing distinct strategies for merging point clouds that contain both sparse and dense points (Holz et al., 2015; S. Li et al., 2016). In sparse-dense point cloud registration, (Lamine Tazir et al., 2018) introduced an innovative algorithm based on local surface characteristics of points, which helps in registering sparse, dense point clouds acquired from different sensors or the same sensor but varying resolution. Their study also entailed a comparative analysis of their algorithm against other state-of-the-art methods, revealing that their approach better superior performance.

On the other hand, Agamennoni et al., (2016) proposed a novel registration algorithm using probability distributions, effective for both sparse-dense and standard point cloud registration tasks. Tazir et al., 2019 introduce a novel approach for sparse dense point cloud registration that improves alignment by clustering points with similar surfaces instead of relying solely on normal features. This method addresses challenges related to varying point cloud densities and noisy sensors. Data enhancing convergence between different depth sensors and increasing alignment precision while reducing computation time, as demonstrated through experiments on real data. This research aims to deploy ICP algorithm, coupled with pre-processing techniques applied to the dataset, to align sparsely and densely sampled point clouds originating from distinct sensors.

Materials and Methods

We conducted experiments in three study sites with a dynamic environment in the context of different features present in the study site, including both indoor and outdoor, employing both the RIEGL VZ-2000 and Velodyne VLP16 sensors to register sparse and dense point clouds. Initially, data was recorded in an enclosed laboratory space with artificial features such as chairs, tables, walls, and computers, followed by data collection in an open urban environment featuring some trees, cars, and buildings. Lastly, data acquisition occurred in a location enclosed by buildings, trees, and parked vehicles.

We have utilized two sensors to capture point clouds of varying density from the same scene. Specifically, we obtained a sparse point cloud using the Velodyne VLP16 sensor and a dense point cloud using the RIEGL VZ-2000 sensor. The RIEGL VZ-2000 sensor excels in generating highly detailed point clouds, capturing intricate geometric information about the environment, while the VLP16 offers a less detailed point cloud but with a higher data rate and is cost-effective (De Sloover et al., 2019; Zhang et al., 2019). Data was acquired at three locations to evaluate the algorithm's robustness.

Following data collection, it was processed and converted into standard point cloud formats using specific software: Veloview for the Velodyne LiDAR output and RiSCAN for the

RIEGL VZ-2000 LiDAR dataset. The sensors' specifications and their setup are mentioned below in Table 1 and Figure 1, respectively.

The methodology is visually presented using a flowchart, showing the steps in registering sparse and dense point clouds (Figure 2). The methodology is generally categorized into two main components: pre-processing, involving data filtering, sampling, and segmentation, and point cloud registration, in which an algorithm is used for merging or aligning the sparse and dense point clouds.

Pre-processing: For the registration process, at least two point clouds are required—one designated as the source and the other as the target or reference point cloud. In this case, we named the VLP-16-based sparse scan as the target point cloud, while the RIEGL VZ-2000-based dense point cloud serves as the reference. The RIEGL VZ-2000 sensor provides notably detailed point clouds compared to the VLP16. Hence, creating significant corresponding pairs between dense to sparse point cloud was difficult. So, reducing the number of points through a resampling process was essential to find its corresponding pairs with the target point cloud. Furthermore, a significant amount of noise and outliers were also present in the dataset, specially in the RIEGL VZ-2000-based point cloud. The filtering technique that was used for this paper was a noise filter. The noise filter locally fits a plane around each point in point cloud data and removes the points far away from the fitted plane. This filter is considered a low-pass filter. A user-defined radius or number of neighbors is considered to estimate the planer surface. There are two types of input we need to provide for filtering. One is the number of neighbor points, and other is the value of the radius. This filter will keep the number of points inside the radius and remove all other points outside the radius. We have provided a radius of 0.2348, and number of neighbor points are 6. As our data set does not have constant density, we provide the value of radius a little bit more, so the sphere should typically capture at least 6 points. Also, we provided the maximum relative error as 1. Suppose we keep a lower value of the radius. In that case, It allows data points with fewer neighbors within the radius to be classified as inliers, potentially making the filter more sensitive to outliers. A higher value of radius results, data points having more neighbors within the radius to be considered inliers, which can make the algorithm more robust to noise (Noise filter, 2023). This filter removes some unwanted noisy points from the data set. Further, some points far away from the experimental site were segmented to achieve the point cloud of the study site only. Finally, we observed significant disparities when merging sparse and dense point clouds generated from various sensors. To align both collected data, substantial shifts in terms of both rotation and translation were necessary. Finally, we observed significant disparities when merging sparse and dense point clouds generated from various sensors. To align both collected data, substantial shifts in terms of both rotation and translation were necessary.

Point cloud registration using ICP: The ICP algorithm computes point-to-point correspondence pairs between two point clouds, iteratively minimizing the distance between them until predefined criteria are satisfied. Finally, it estimates the transformation matrix required to align the two point clouds. This algorithm is implemented for the coarse–sparse point cloud registration after pre-processing. For this, both the point clouds are roughly aligned together, and ICP is performed (Li et al., 2020).

Table 1. Characteristics of the LiDAR sensors used for the experiments.

Specification	Velodyne VLP16	Riegl VZ-2000
Channels	16	1
Range	100 m	2500 m
Vertical FOV	$+15^0$ to -15^0 (30^0)	100^0
Horizontal FOV	360^0	360^0
Vertical angular resolution	2.0^0	0.0007^0
Horizontal angular resolution	$0.1^0 - 0.4^0$	0.0015
Range accuracy	±0.03 m	±0.005 m
Points per second (max)	396,000	500,000

Fig. 1 Experimental setup for (a) RIEGL VZ-2000 and (b) Velodyne VLP16.

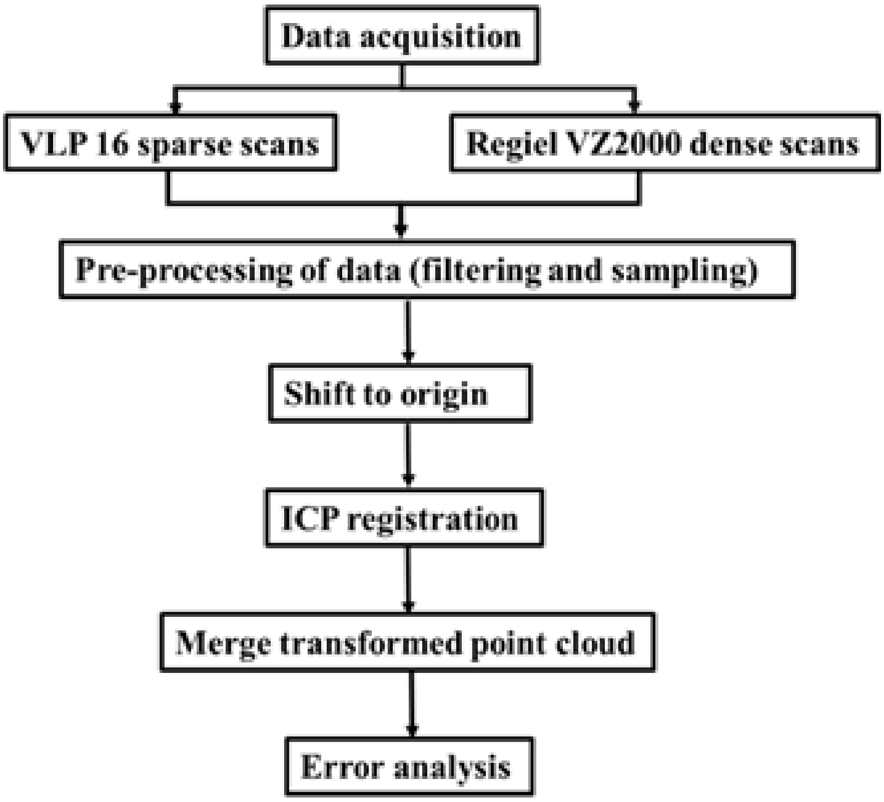

Fig. 2 Overall methodology flowchart for sparse, dense point cloud registration.

The steps for registration are mentioned below:

1. The corresponding pair has been created for each point in the source point cloud S by searching the nearest point in the target point cloud T.
2. The source point cloud's coordinate system is transformed to align with the target point cloud. This results in a rigid transformation matrix that quantifies the necessary translation and rotation to align the source point cloud with the target point cloud.
3. Error Analysis

Error analysis in point cloud registration primarily aims to assess the level of alignment accuracy between two-point clouds. Registration accuracy is typically quantified by computing the offset distance between model point clouds and registration point clouds following the transformation process (Cheng et al., 2018).

We determined the threshold value and iterated the algorithm until the value of RMSE between S and T was less than a threshold (equation 1).

$$\text{RMSE} = \sqrt{\frac{1}{n}\sum_{i=1}^{n}\left(s_i - t_j\right)^2} < \sigma, \ (1 \leq j \leq m) \qquad (1)$$

where s_i is the nearest point in the target dataset of t_j in the source dataset, m and n are the numbers of S and T, respectively, respectively, and σ is the threshold for minimum distance between the two datasets.

Results

This section describes the experiments and results of this research. 3-D point cloud has been created for 3 study sites to test the algorithm's robustness for sparse and dense point cloud registration. This section shows registration results for two experimental sites only, as similar featured environments surrounded 2nd and 3rd study sites. Additionally, the RMSE graph is also shown in the form of a graph.

Result of pre-processing: After pre-processing, the size of the dataset, especially from RIEGL VZ-2000, are reduced significantly due to the longer-range data capturing of the instrument, so it was removed using a filtering technique. Conversely, there was not much reduction of the number of points observed in the VLP16 after pre-processing as there was not much data found beyond the study site due to the shorter range of the VLP16 (table 2).

Table 2 shows the number of points in the point cloud before pre-processing (raw point cloud recorded in the field) and after pre-processing.

	Before pre-processing (no. of points)		**After pre-processing (no. of points)**	
	RIEGL VZ-2000	**VLP16**	**RIEGL VZ-2000**	**VLP16**
Enclosed laboratory site	15639538	13439	297498	13299
Open built-up site	13488213	14528	603695	14095

Result of point cloud registration: This section provides the outcomes of our point cloud registration efforts for two distinct study sites. We have presented these results in two formats: first, through a figure that visually illustrates the registration process, and second, by including an analysis of the Root Mean Square Error (RMSE) and an accuracy assessment.

The RMSE values have been analyzed, and this analysis is visually represented in the form of a plot.

Results of the registration process conducted in the enclosed laboratory environment: After pre-processing, we obtained the initial coarsely registered point cloud as depicted in Figure 3, which was used as an input for the final registration algorithm ICP. Figure 4a is the final registered point cloud, which depicts the alignment between the sparse and dense point cloud. The results revealed a tight alignment of the walls after registering the sparsely sampled Velodyne point cloud (indicated in yellow) with the densely sampled RIEGL VZ-2000 point cloud indicated in pink color (figure 4a). Certain features, such as the room's wall and the edge of the desk, are emphasized to demonstrate effective registration, as shown in Figure 4b and Figure 4c, respectively. Notably, the sparse point cloud contains significantly fewer points than the dense point cloud achieved from RIEGL VZ-2000, hence it cannot represent all the features of the study site. Additionally, the Root Mean Square (RMS) deviation, computed on 132,399 points, is estimated as 0.046 m, indicating a high degree of alignment precision between the point clouds.

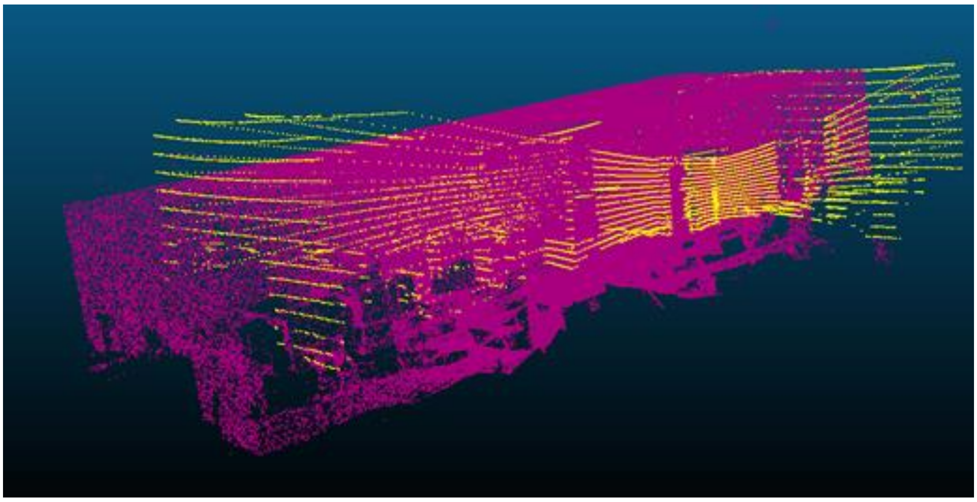

Fig. 3 Input point clouds before registration in the enclosed laboratory environment after pre-processing.

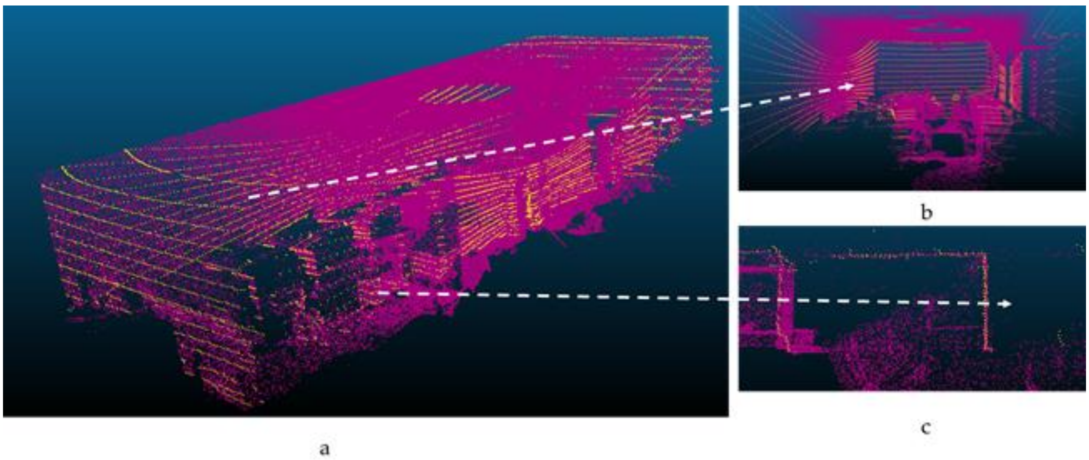

Fig. 4 Input Point cloud after Registration in the enclosed laboratory environment (figure. 4a). Figure. 4b shows a side view of the room (wall of the room) and figure. 4c shows the edge of the desk.

Results of the registration process conducted in an open built-up environment: The identical procedure was employed for point cloud registration within an open built-up environment. Figure 5 depicts the initial point clouds used for registration, generated after pre-processing, where the sparse point cloud is shown in green color and the dense point cloud in yellow color. The final registered point cloud, achieved through the ICP algorithm, demonstrates the successful alignment of walls, poles, and cars, as depicted in Figure 6a. It is worth noting that some minor deviations along the horizontal direction were observed in the alignment of trees, persisting even after registration, as shown in Figure 6b. Figure 6c and Figure 6d highlight the well-aligned artificial features such as boundary walls and cars as these are planar features. Further, the calculated RMS error was 0.36 m, computed on 14,095 points, signifying the level of alignment precision.

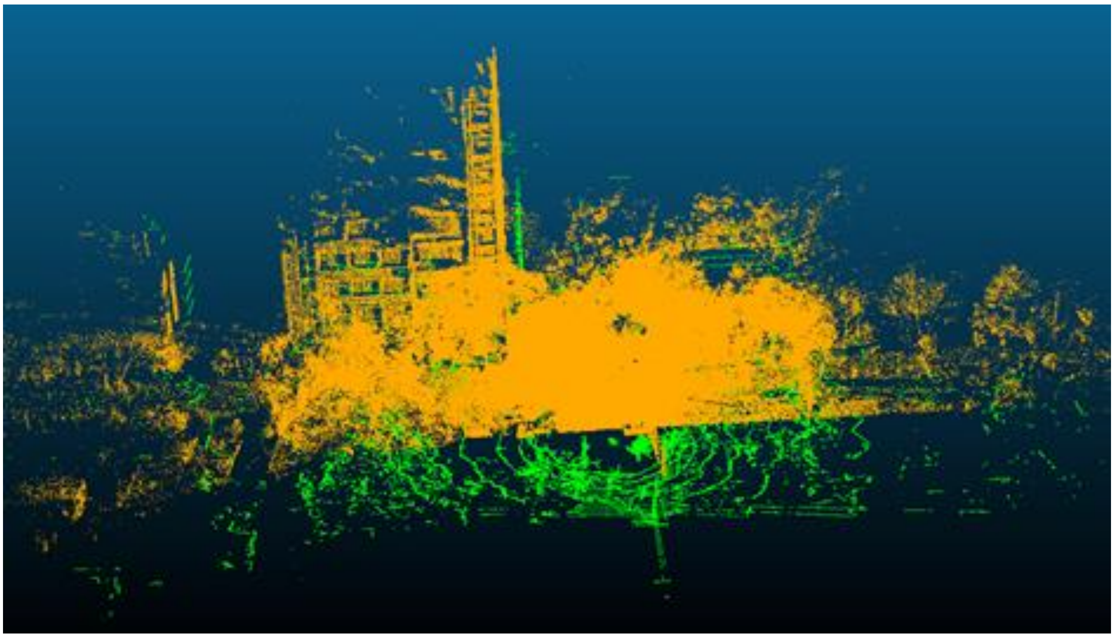

Fig. 5 Input point cloud for the open built-up environment before registration (after pre-processing).

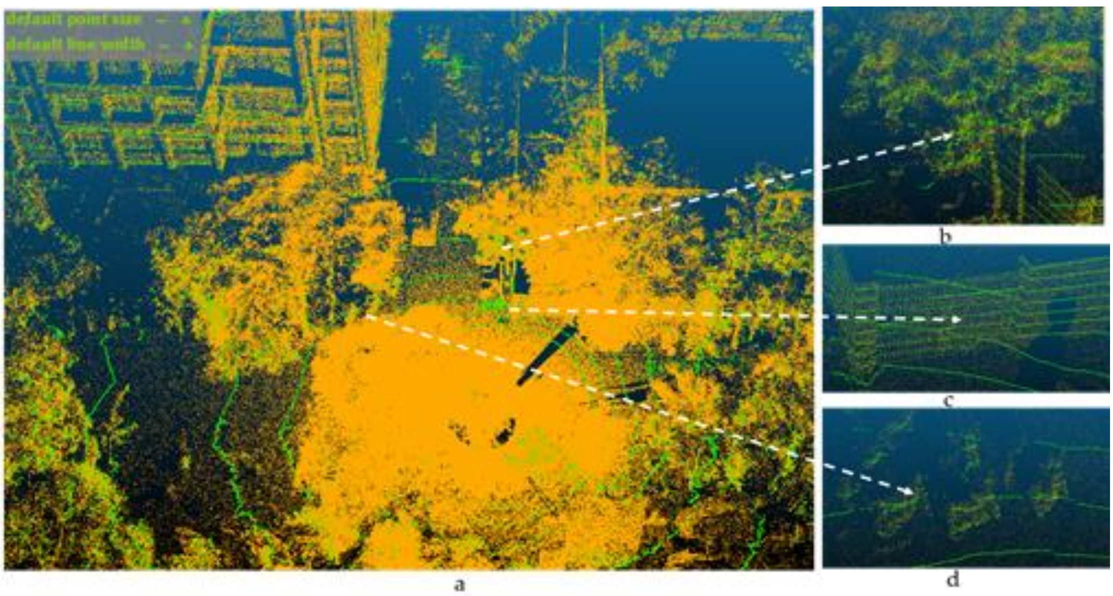

Fig. 6 Aligned/registered point cloud after registration in open built-up environment (figure. 6a). Figure 6b, figure 6c, and figure 6d shows the tree, boundary wall, and vehicles.

Accuracy analysis: A RMSE plot has been generated based on the number of iterations (figure 7). The data represents the Root Mean Square Error (RMSE) values at different numbers of iterations for point cloud registration in two different environments: "Laboratory Space" and "Open Built-up Space". In the plot, X- axes represent the number of iteration while Y-axes represent the corresponding RMSE value. RMSE value decreases with increasing number of iterations for both the site up to certain number of iterations. RMSE gets saturated after 20 iterations in case of Laboratory space while for open built-up space, RMSE fluctuates with minimal deviation after 15 iterations. Further, we observe that RMSE is higher for Open built-up sites with respect to Laboratory space.

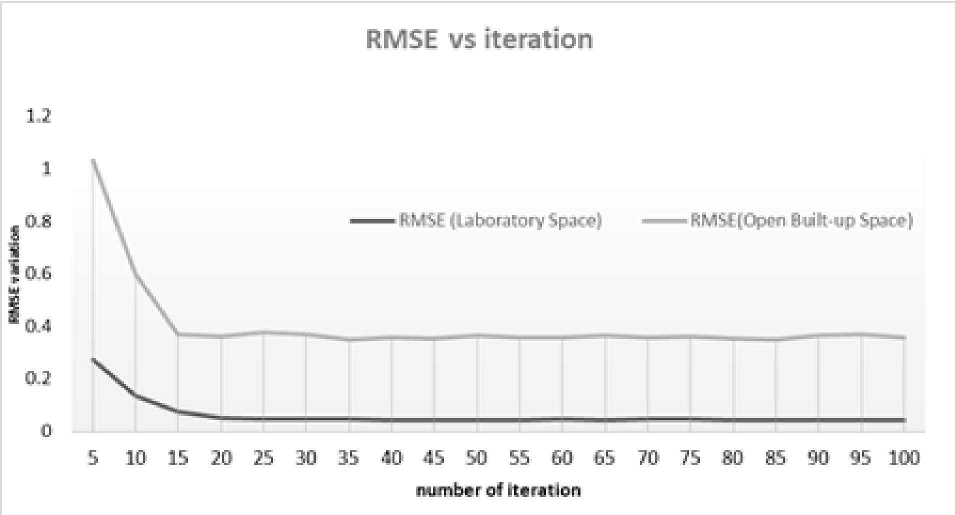

Fig. 7 The plot represents the RMSE vs iteration plots.

Discussion

In the ICP point cloud registration results across two experimental areas, enclosed laboratory areas with distinct geometric or planar features exhibit strong alignment. In contrast, another experimental site, such as open areas with trees or other natural features, showed poorer alignment, as confirmed by higher RMSE values. Our analysis discovered a noteworthy distinction in the Root Mean Square Error (RMSE) values, with the lowest RMSE occurring within enclosed laboratory spaces compared to other open built-up environments. Additionally, from the RMSE plot (figure 7), we noted that the RMSE reaches a saturation point after a certain number of iterations in both study sites. This saturation point implies that increasing the number of iterations does not significantly increase or decrease RMSE. Consequently, there is no advantage in extending the iteration count beyond this saturation point to attain an optimal RMSE, as it stabilizes and ceases to improve beyond a certain threshold. This discrepancy in RMSE values can be attributed to the nature of the corresponding point pairs used for registration. Furthermore, we observed that, in enclosed laboratory spaces, the corresponding pairs used for registration predominantly originate from planar surfaces or specific geometric features. These environments provide well-defined and easily identifiable reference points, resulting in more accurate and tightly aligned point clouds (figure 4). Conversely, in open built-up environments, the sources for corresponding point pairs are often less structured. These can include trees, vegetation, or other non-geometric elements lacking the distinct geometric characteristics of enclosed built-up spaces (figure 6). Consequently, the registration process in open built-up environments encounters more significant challenges, leading to higher RMSE values (figure 7). This observation highlights the importance of considering the environmental features when assessing the effectiveness of point cloud registration algorithms. It also highlights the need for specialized approaches or adaptations when dealing with point clouds from open and less structured environments.

Conclusions

In this paper, we have successfully demonstrated the effectiveness of our approach, which combines the ICP algorithm with pre-processing techniques for registering sparse and dense point clouds from different sensors. It acknowledges variations in RMSE based on the environment and suggests that the method can be applied to various applications. It provides valuable insights into the potential and limitations of the proposed approach and highlights the importance of considering the environment when assessing registration accuracy. In future research on sparse-dense point cloud registration, it is worthwhile to explore various iterations of the ICP algorithm and improve the accuracy of the registration so that it can be used for the localization of robots, calibrations of sensors, and other applications.

Acknowledgments

This work is partially supported by the Start-up Research Grant of SERB (SRG/2020/000193). The authors would like to acknowledge the support received from SERB, India.

References

Agamennoni, G., Fontana, S., Siegwart, R. Y., & Sorrenti, D. G. (2016). Point cloud registration with probabilistic data association. In 2016 IEEE/RSJ International Conference on Intelligent Robots and Systems (IROS), IEEE, 4092-4098, 9-14, Daejeon, Korea.

Bellekens, B., Spruyt, V., Berkvens, R., & Weyn, M. (2014). A survey of rigid 3d point cloud registration algorithms. In AMBIENT 2014: the Fourth International Conference on Ambient Computing, Applications, Services and Technologies, 8-13, 24-28 August, Rome, Italy.

Besl, P. J., & McKay, N. D. (1992). A Method for Registration of 3-D Shapes. IEEE Transactions on Pattern Analysis and Machine Intelligence, 14(2).

Brenner, C., Dold, C., & Ripperda, N. (2008). Coarse orientation of terrestrial laser scans in urban environments. ISPRS journal of photogrammetry and remote sensing, 63(1), 4-18.

Brightman, N., Fan, L., & Zhao, Y. (2023). Point cloud registration: A mini-review of the current state, challenging issues, and future directions. AIMS Geosci, 9, 68-85.

Cheng, L., Chen, S., Liu, X., Xu, H., Wu, Y., Li, M., & Chen, Y. (2018). Registration of laser scanning point clouds: A review. Sensors, 18(5), 1641.

De Reu, J., De Smedt, P., Herremans, D., Van Meirvenne, M., Laloo, P., & De Clercq, W. (2014). On introducing an image-based 3D reconstruction method in archaeological excavation practice. Journal of Archaeological Science, 41, 251-262.

De Sloover, L., De Wulf, A., Stal, C., Verbeurgt, J., & Vos, S. (2019). Case Study of a Hypertemporal Terrestrial LiDAR to Monitor a Macrotidal Beach: Assessment of Different Calibration Procedures. International Multidisciplinary Scientific GeoConference: SGEM, 57-64, 28 June - 07 July, Albena, Bulgeria.

Han, J., Yin, P., He, Y., & Gu, F. (2016). Enhanced ICP for the registration of large-scale 3D environment models: An experimental study. Sensors, 16(2), 228.

He, Y., Yang, J., Hou, X., Pang, S., & Chen, J. (2021). ICP registration with DCA descriptor for 3D point clouds. Optics express, 29(13), 20423-20439.

Holz, D., Ichim, A. E., Tombari, F., Rusu, R. B., & Behnke, S. (2015). Registration with the point cloud library: A modular framework for aligning in 3-D. IEEE Robotics & Automation Magazine, 22(4), 110-124.

Huang, X., Mei, G., Zhang, J., & Abbas, R. (2021). A comprehensive survey on point cloud registration. arXiv preprint arXiv:2103.02690.

Kelbe, D., Van Aardt, J., Romanczyk, P., Van Leeuwen, M., & Cawse-Nicholson, K. (2016). Marker-free registration of forest terrestrial laser scanner data pairs with embedded confidence metrics. IEEE transactions on geoscience and remote sensing, 54(7), 4314-4330.

Li, P., Wang, R., Wang, Y., & Gao, G. (2019). Fast method of registration for 3D RGB point cloud with improved four initial point pairs algorithm. Sensors, 20(1), 138.

Li, P., Wang, R., Wang, Y., & Tao, W. (2020). Evaluation of the ICP algorithm in 3D point cloud registration. IEEE Access, 8, 68030-68048.

Li, S., Wang, J., Liang, Z., & Su, L. (2016). Tree point clouds registration using an improved ICP algorithm based on kd-tree. In 2016 IEEE International Geoscience and Remote Sensing Symposium (IGARSS) IEEE, 10-15 July, Beijing, China.

Li, W., & Song, P. (2015). A modified ICP algorithm based on dynamic adjustment factor for registration of point cloud and CAD model. Pattern Recognition Letters, 65, 88-94.

Noise filter https://www.cloudcompare.org

Pomerleau, F., Colas, F., & Siegwart, R. (2015). A review of point cloud registration algorithms for mobile robotics. Foundations and Trends® in Robotics, 4(1), 1-104.

Sanchez, J., Denis, F., Checchin, P., Dupont, F., & Trassoudaine, L. (2017). Global registration of 3D LiDAR point clouds based on scene features: Application to structured environments. *Remote Sensing*, *9*(10), 1014.

Tazir, M. L., Gokhool, T., Checchin, P., Malaterre, L., & Trassoudaine, L. (2018). CICP: Cluster Iterative Closest Point for sparse–dense point cloud registration. Robotics and Autonomous Systems, 108, 66-86.

Tazir, M. L., Gokhool, T., Checchin, P., Malaterre, L., & Trassoudaine, L. (2019). Cluster ICP: Towards sparse to dense registration. In Intelligent Autonomous Systems 15: Proceedings of the 15th International Conference IAS-15, 730-747.

Wang, X., Yang, Z., Cheng, X., Stoter, J., Xu, W., Wu, Z., & Nan, L. (2023). GlobalMatch: Registration of forest terrestrial point clouds by global matching of relative stem positions. ISPRS Journal of Photogrammetry and Remote Sensing, 197, 71-86.

Xu, N., Qin, R., & Song, S. (2023). Point cloud registration for LiDAR and photogrammetric data: A critical synthesis and performance analysis on classic and deep learning algorithms. ISPRS open journal of photogrammetry and remote sensing, 100032.

Xu, X., Wang, P., Gan, X., Sun, J., Li, Y., Zhang, L., ... & Li, X. (2022). Automatic marker-free registration of single tree point-cloud data based on rotating projection. Artificial Intelligence in Agriculture, 6, 176-188.

Yang, J., Li, H., Campbell, D., & Jia, Y. (2015). Go-ICP: A globally optimal solution to 3D ICP point-set registration. IEEE transactions on pattern analysis and machine intelligence, 38(11), 2241-2254.

Zhang, J., Zhang, R., Yue, Y., Yang, C., Wen, M., & Wang, D. (2019). Slat-calib: Extrinsic calibration between a sparse 3d lidar and a limited-fov low-resolution thermal camera. In 2019 IEEE international conference on robotics and biomimetics (ROBIO), IEEE, 648-653, 06-08 December, Yunnan, China.

Citation

Barnwal, S., Goel, S., Koshti, M.P. (2024). Registration of Sparse-Dense Point Cloud from LiDAR and its Applications. In: Dandabathula, G., Bera, A.K., Rao, S.S., Srivastav, S.K. (Eds.), Proceedings of the 43rd INCA International Conference, Jodhpur, 06–08 November 2023, pp. 499–509, ISBN 978-93-341-2277-0.